Behavioural Brain Research 255 (2013) 64–74

Contents lists available at ScienceDirect

Behavioural Brain Research

journal homepage: www.elsevier.com/locate/bbr

Research report

Long-lasting silencing of orexin/hypocretin neurons using archaerhodopsin induces slow-wave sleep in mice☆

Tomomi Tsunematsu[a,b], Sawako Tabuchi[a,b,c], Kenji F. Tanaka[d], Edward S. Boyden[e], Makoto Tominaga[a,c], Akihiro Yamanaka[a,f,g,*]

[a] Division of Cell Signaling, Okazaki Institute for Integrative Bioscience, National Institute for Physiological Sciences, Okazaki 444-8787, Japan
[b] The Japan Society for the Promotion of Sciences, Tokyo 102-8472, Japan
[c] Department of Physiological Sciences, The Graduate University for Advanced Studies, Okazaki 444-8787, Japan
[d] Department of Neuropsychiatry, School of Medicine, Keio University, Tokyo 160-8582, Japan
[e] Department of Biological Engineering, Massachusetts Institute of Technology, Cambridge, MA 02139, USA
[f] Department of Neuroscience II, Research Institute of Environmental Medicine, Nagoya University, Nagoya 464-8601, Japan
[g] PRESTO, JST, Kawaguchi 332-0012, Japan

HIGHLIGHTS

- New transgenic mice, TetO archaerhodopsin (ArchT) BAC mice, were generated.
- Specific expression of ArchT was confirmed by breeding with *orexin-tTA* mice.
- Slice patch clamp confirmed that green light illumination silenced orexin neurons.
- One hour silencing of orexin neurons induced slow-wave sleep in the dark period.

ARTICLE INFO

Article history:
Received 17 December 2012
Received in revised form 8 April 2013
Accepted 14 May 2013
Available online 21 May 2013

Keywords:
Orexin
Hypocretin
Optogenetic
Archaerhodopsin
Slow-wave sleep

ABSTRACT

Orexin/hypocretin neurons have a crucial role in the regulation of sleep and wakefulness. Recent optogenetic studies revealed that the activation or inhibition of orexin neuronal activity affects the probability of sleep/wakefulness transition in the acute phase. To expand our understanding of how orexin neurons maintain wakefulness, we generated new transgenic mice in which orexin neurons expressed archaerhodopsin from Halorubrum strain TP009 (ArchT), a green light-driven neuronal silencer, using the tet-off system (*orexin-tTA; TetO ArchT* mice). Slice patch clamp recordings of ArchT-expressing orexin neurons demonstrated that long-lasting photic illumination was able to silence the activity of orexin neurons. We further confirmed that green light illumination for 1 h in the dark period suppressed orexin neuronal activity *in vivo* using c-Fos expression. Continuous 1 h silencing of orexin neurons in freely moving *orexin-tTA; TetO ArchT* mice during the night (the active period, 20:00–21:00) significantly increased total time spent in slow-wave sleep (SWS) and decreased total wake time. Additionally, photic inhibition increased sleep/wakefulness state transitions, which is also evident in animals lacking the prepro-orexin gene, orexin neurons, or functional orexin-2 receptors. However, continuous 1 h photic illumination produced little effect on sleep/wakefulness states during the day (the inactive period, 12:00–13:00). These results suggest that orexin neuronal activity plays a crucial role in the maintenance of wakefulness especially in the active phase in mice.

1. Introduction

Orexin A and B (or hypocretin-1 and hypocretin-2) are a pair of neuropeptides expressed in a specific population of neurons in the lateral hypothalamic area (LHA) [1,2]. Animals that lack the orexin peptide (*prepro-orexin* knockout mice), orexin neurons (*orexin/ataxin-3* transgenic mice), or functional orexin 2 receptors (OX2Rs, *via* OX2R knockout mice and OX2R mutated dogs) show phenotypes remarkably similar to those of the human sleep disorder, narcolepsy [3–6]. Narcoleptic patients show symptoms of

* Corresponding author at: Department of Neuroscience II, Research Institute of Environmental Medicine, Nagoya University, Nagoya 464-8601, Japan. Tel.: +81 52 789 3864; fax: +81 52 789 3889.
E-mail address: yamank@riem.nagoya-u.ac.jp (A. Yamanaka).

0166-4328/$ – see front matter © 2013 The Authors. Published by Elsevier B.V. All rights reserved.
http://dx.doi.org/10.1016/j.bbr.2013.05.021

fragmented sleep and wakefulness, sleep-onset rapid eye movement (REM), and cataplexy, a sudden bilateral postural muscle weakness usually precipitated by emotional stimuli. In addition, the concentration of orexin-A (hypocretin-1) peptide in the cerebrospinal fluid (CSF) of narcoleptic patients is greatly reduced [7], and a specific degeneration of orexin neurons has also been reported [8,9]. Indeed, central administration of orexin induces wakefulness and decreases slow-wave sleep (SWS) and REM sleep durations [10,11]. Orexin neurons are thought to be phasically active during wakefulness and silent during SWS [12–14]. These findings indicate that the orexin system plays a crucial role in the regulation of sleep/wakefulness, especially in the maintenance of arousal.

Orexin neurons project throughout the brain and densely innervate monoaminergic nuclei, including the dorsal raphe nucleus (DR), locus coeruleus (LC) and tuberomammillary nucleus (TMN) [1,15,16]. These monoaminergic nuclei are implicated in increasing arousal and promoting wakefulness. The activity of monoaminergic neurons in the DR, LC and TMN is synchronized and strongly associated with sleep/wakefulness states [17–20]. That is, these neurons exhibit tonic firing during wakefulness, decreased firing during SWS, and electrical quiescence during REM sleep. Electrophysiological experiments have shown that serotonergic cells in the DR, noradrenergic cells in the LC and histaminergic cells in the TMN are activated by orexin *via* the activation of orexin 1 receptors (OX1Rs) and/or OX2Rs [21–24]. On the other hand, GABAergic neurons in the ventrolateral preoptic area (VLPO) seem to play a crucial role in sleep initiation and maintenance. Neurons in the VLPO exhibit high frequency firing during sleep, whereas they display less firing during wakefulness [25–27]. Orexin neurons are innervated by GABAergic neurons in the VLPO [28], and are strongly hyperpolarized by muscimol or baclofen, a $GABA_A$ receptor agonist or a $GABA_B$ receptor agonist, respectively [29,30]. Sleep-promoting GABAergic neurons in the VLPO and arousal-promoting monoaminergic neurons in the DR, LC and TMN project reciprocally and mutually inhibit each other's activity [31]. As such, these neuronal circuitries are important for the regulation of sleep/wakefulness. In particular, orexin neurons have a crucial role in the maintenance of wakefulness by modulating the mutual inhibition because elimination of orexin neurons results in fragmentation of sleep/wakefulness as displayed in narcolepsy.

Recent studies using optogenetics have demonstrated the importance of orexin neuronal activity in the regulation of sleep and wakefulness states. Activation of orexin neurons *via* channelrhodopsin-2 (ChR2), a blue light-activated, non-selective cation channel, or melanopsin, a blue light-activated Gq type of G-protein coupled receptor, increases the probability of transitions to wakefulness from SWS and REM sleep in mice [32–34]. In contrast, acute inhibition of orexin neurons *via* halorhodopsin (HaloR), an orange light-driven chloride pump, promotes the transition to SWS from wakefulness [35]. These results directly establish a causal link between activity of orexin neurons and sleep/wakefulness transition. However, technical limitations of the first generation of optogenetics make it difficult to control the activity of neurons for extended periods.

To address this, we generated new transgenic mice in which orexin neurons express Archaerhodopsin T (ArchT), a green light-driven powerful neuronal silencer. ArchT was recently discovered from *Halorubrum* strain TP009 and forms proton pumps suitable for complete silencing [36]. Using these mice, we were able to continuously inhibit orexin neurons *in vitro* and *in vivo*. We found that *in vivo* inhibition of orexin neurons for 1 h increased time spent in SWS and decreased time spent in wakefulness only during the dark period. This result suggests that orexin neuronal activity plays an important role in the maintenance of wakefulness, especially in the active phase.

2. Methods

2.1. Animal usage

All experimental procedures involving animals were approved by the National Institute for Physiological Sciences Animal Care and Use Committee and were in accordance with NIH guidelines. All efforts were made to minimize animal suffering or discomfort and to reduce the number of animals used.

2.2. Generation of TetO ArchT BAC transgenic mice

To generate the TetO ArchT BAC transgenic mice, an archaerhodopsin cDNA fragment from Halorubrum strain TP009 (ArchT) [36] was swapped with that of the ChR2(C128S) sequence in *TetO ChR2(C128S)EGFP-Neo* construct flanked on both sides by a β-actin gene homology arm [37]. BAC DNA (clone RP23-289L7) was modified by BAC recombination with this transgene with homology arms, resulting in the insertion of *TetO ArchT-EGFP-Neo* cassette 30 bp downstream of a mouse β-actin polyA signal. To remove the FRT-flanked Neo cassette, recombined BAC DNA was electroporated into strain SW105 (kindly gifted from Dr. Neal Copeland, National Cancer Institute) that possesses flippase activity. Linearized modified BAC DNA was injected into fertilized eggs from C57BL/6J (Clea-Japan Inc., Tokyo, Japan) mice. Founders were bred with C57BL/6J mice to produce stable *TetO ArchT* transgenic lines. A total of 3 *TetO ArchT* transgene-positive founders were obtained. We crossed these mice with *orexin-tTA* mice [38] to obtain orexin neuron-specific ArchT-EGFP-expressing mice (see Fig. 1). Immunohistochemical analysis of the N1 generation revealed that line A showed the highest EGFP expression (see Fig. 2). Thus, line A was used for further experimentation.

2.3. Brain slice preparation

Male and female *orexin-tTA; TetO ArchT* double transgenic mice (3–4 weeks old) were used for whole cell recordings. The mice were deeply anesthetized with isoflurane (Abbott Japan, Tokyo, Japan) and decapitated. Brains were quickly isolated in ice-cold cutting solution consisting of (in mM): 280 sucrose, 2 KCl, 10 HEPES, 0.5 $CaCl_2$, 10 $MgCl_2$, 10 glucose, pH 7.4 with NaOH, bubbled with 100% O_2. Brains were cut coronally into 350 μm slices with a microtome (VTA-1200S, Leica, Wetzlar, Germany). Slices containing the LHA were transferred to an incubation chamber shielded from light and filled with a physiological solution containing (in mM): 135 NaCl, 5 KCl, 1 $CaCl_2$, 1 $MgCl_2$, 10 HEPES, 10 glucose, pH 7.4 with NaOH, bubbled with 100% O_2 and incubated for at least 1 h at room temperature (RT; 24–26 °C).

2.4. Electrophysiological recordings

At RT, the slices were transferred to a recording chamber (RC-27L, Warner Instrument Corp., CT) on a fluorescence microscope stage (BX51WI, Olympus, Tokyo, Japan). Neurons having EGFP fluorescence were identified as orexin neurons and were subjected to electrophysiological recordings. The fluorescence microscope was equipped with an infrared camera (C2741-79, Hamamatsu Photonics, Hamamatsu, Japan) for infrared differential interference contrast (IR-DIC) imaging and a cooled charge-coupled device (CCD) camera (Cascade 650, Roper Scientific, Tucson, AZ) for fluorescent imaging. Each image was displayed separately on a monitor and saved on a computer. Recordings were carried out with an Axopatch 200B amplifier (Axon Instruments, Foster City, CA) using a borosilicate pipette, (GC150-10, Harvard Apparatus, Holliston, MA) prepared by a micropipette puller (P-97, Sutter Instruments, Novato, CA), and filled with intracellular solution (4–6 MΩ) consisting of (in mM): 138 K-gluconate, 10 HEPES, 8 NaCl, 0.2 EGTA-Na_3, 2 MgATP, 0.5 Na_2GTP, pH 7.3 with KOH. The osmolality of the solution was checked by a vapor pressure osmometer (model 5520, Wescor, Logan, UT). The osmolality of the internal and external solutions was 280–290 and 320–330 mOsm/L, respectively. The liquid junction potential of the patch pipette and perfused extracellular solution was estimated to be 16 mV and was corrected in the data. Recording pipettes were under positive pressure while advancing toward individual cells in the slice, and tight seals on the order of 1.0–1.5 GΩ were made by negative pressure. The membrane patch was then ruptured by suction. The series resistance during recording was 10–25 MΩ. The reference electrode was an Ag–AgCl pellet immersed in bath solution. During recordings at RT, cells were superfused with extracellular solution at a rate of 1.6 mL/min using a peristaltic pump (Dynamax, Rainin, Oakland, CA). Green light (549 ± 7.5 nm) was generated by lumencor (SPECTRA light engine, Lumencor. Inc., OR, USA).

The output signal was low-pass filtered at 5 kHz and digitized at 10 kHz. Data were recorded on a computer through a Digidata 1322A A/D converter using pClamp software version 10.2 (Axon Instruments, Union City, CA).

2.5. Drugs

Tetrodotoxin (TTX) (Wako, Osaka, Japan) was dissolved in extracellular solution at a concentration of 1 μM. During the experiments, TTX was applied by bath application.

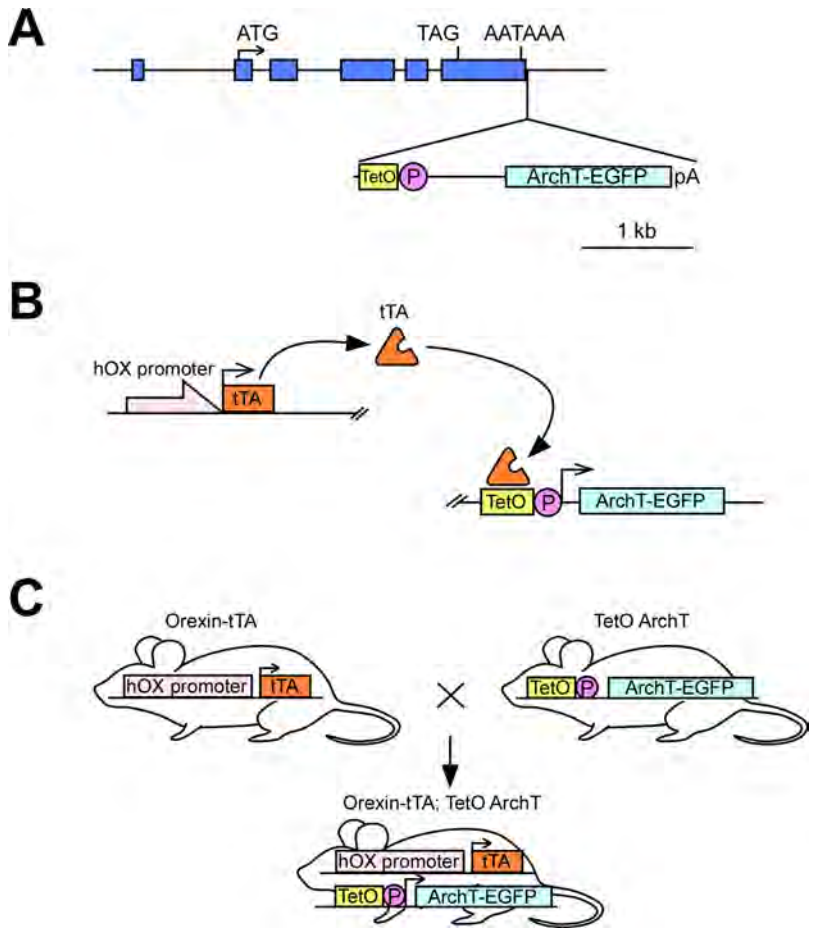

Fig. 1. Generation of *orexin-tTA; TetO ArchT* double-transgenic mouse. (A) Structure of *TetO ArchT* BAC transgene. There is the sequence of tetracycline operater (TetO, yellow square), which binds tTA protein, and minimal promoter (P, circle) in 0.7 kb upstream of *ArchT-EGFP* (light blue square). The β-actin gene consists of 6 exons (blue squares), and the *TetO ArchT* cassette is inserted just downstream of the polyadenylation signal of the β-actin gene. (B) Schematic illustration of the tetracycline-controlled gene expression system and tTA-induced ArchT expression in orexin neurons. (C) Schema indicating how *orexin-tTA* mice are bred with *TetO ArchT* mice to generate double-transgenic mice, *orexin-tTA; TetO ArchT* mice. hOX promoter, human prepro-orexin promoter. P, minimal promoter. TetO, tetracycline operator. tTA, tetracycline-controlled transcriptional activator. (For interpretation of the references to color in this figure legend, the reader is referred to the web version of the article.)

2.6. Immunohistochemistry

Male and female *orexin-tTA; TetO ArchT* transgenic mice (6 weeks old) were deeply anesthetized with isoflurane and perfused sequentially with 20 mL of chilled saline and 20 mL of chilled 10% formalin solution (Wako). The brains were removed and immersed in the above fixative solution for 24 h at 4 °C and then immersed in a 30% sucrose solution for at least 2 days. The brains were quickly frozen in embedding solution (Sakura Finetechnical Co. Ltd., Tokyo, Japan). For orexin and GFP double-staining, coronal sections (40 μm) of *orexin-tTA; TetO ArchT* transgenic mice brains were incubated with mouse anti-GFP antiserum (1/1000, Wako) for 24 h at 4 °C. These sections were incubated with Alexa 488-labeled donkey anti-mouse IgG (1/1000, Biotium, CA, USA) for 1 h at RT. The sections were then incubated with goat anti-orexin antiserum (1/1000, Santa Cruz Biotechnology, CA, USA) for 24 h at 4 °C and incubated with Alexa 594-labeled donkey anti-goat IgG (1/1000, Biotium) for 1 h at RT. The sections were mounted and examined with a fluorescence microscope (BZ-9000, Keyence, Osaka, Japan).

For orexin and c-Fos double staining, coronal sections (40 μm) were stained by the avidin-biotin-peroxidase method. Brain sections were incubated for 40 min in phosphate-buffered saline (PBS) containing 0.3% H_2O_2 to inactivate endogenous peroxidase. Sections were transferred into PBS containing 0.25% Triton X-100 and 1% bovine serum albumin fraction V (PBS-BX) for 30 min and then incubated with rabbit anti-c-Fos antibody (AB5, Calbiochem, Billerica, MA, USA) diluted 1/6000 in PBS-BX overnight at 4 °C. Sections were then incubated with biotin labeled anti-rabbit IgG goat antibody (Vector Laboratories, Burlingame, CA) for 1 h at RT followed by incubation with avidin and biotinylated peroxidase complex solution for 1 h at RT. Bound peroxidase was visualized by incubating sections with 0.01 M imidazole acetate buffer containing 0.05% 3,3-diaminobenzidine tetrahydrochloride (Dako, Carpinteria, CA), 0.0015% H_2O_2 and 2.5% nickel ammonium sulfate, which resulted in a black reaction product. For double-labeling, sections were incubated overnight at 4 °C with guinea pig anti-orexin antibody diluted 1/800 in PBS-BX. Sections were then incubated with biotin labeled anti-guinea pig IgG goat antibody (Vector Laboratories) for 1 h at RT. Bound peroxidase was visualized by DAB-buffer tablet (Merck, NJ) with 0.0015% H_2O_2, resulting in a golden-brown reaction product. The sections were mounted and examined with a microscope (BZ-9000, Keyence) or a confocal microscope (LSM710, Zeiss, Germany). To confirm the specificity of antibodies, incubations without primary antibody were conducted as a negative control in each experiment and in each case no signal was observed.

2.7. In vivo photo illumination using freely moving mice

15-Week-old male *orexin-tTA; TetO ArchT* transgenic mice were housed under controlled lighting (12 h light/dark cycle; lights on from 8:00 to 20:00) and temperature (22 °C) conditions. Food and water were available *ad libitum*. Mice were anesthetized with isoflurane using a vaporizer for small animals (400, Bio Research Center Co. Ltd., Nagoya, Japan) and positioned in a stereotaxic frame (David Kopf Instruments, Tujunga, CA). Plastic fiber optics (0.5 mm in diameter; Eska, Mitsubishi Rayon Co. Ltd., Tokyo, Japan) were bilaterally implanted into the hypothalamus approximately 1 mm above the LHA (1.2 mm posterior, 1 mm lateral from bregma, 3.5 mm depth from brain surface). Electrodes for EEG and EMG were implanted on the skull and neck muscle, respectively. These were attached to the skull using dental cement (GC Corporation, Tokyo, Japan). The mice were then housed separately for a recovery period of at least 7 d.

Continuous EEG and EMG recordings were carried out through a slip ring (Air Precision, Le Pressis Robinson, France) designed so that the movement of the mouse was unrestricted. EEG and EMG signals were amplified (AB-610J, Nihon Koden, Tokyo, Japan), filtered (EEG, 1.5–30 Hz; EMG, 15–300 Hz), digitized at a sampling rate of 128 Hz, and recorded using SleepSign software version 3 (Kissei Comtec, Nagano, Japan). Green light (542 ± 13.5 nm) was generated by Lumencor and applied through plastic optical fibers bilaterally inserted 1 mm above the LHA. An optical swivel (COME2, Lucir, Tsukuba, Japan) was used for unrestricted *in vivo* photo illumination. Green light power intensity at the tip of the plastic fiber optics (0.5 mm diameter) was 23 mW/mm^2 as measured by a power

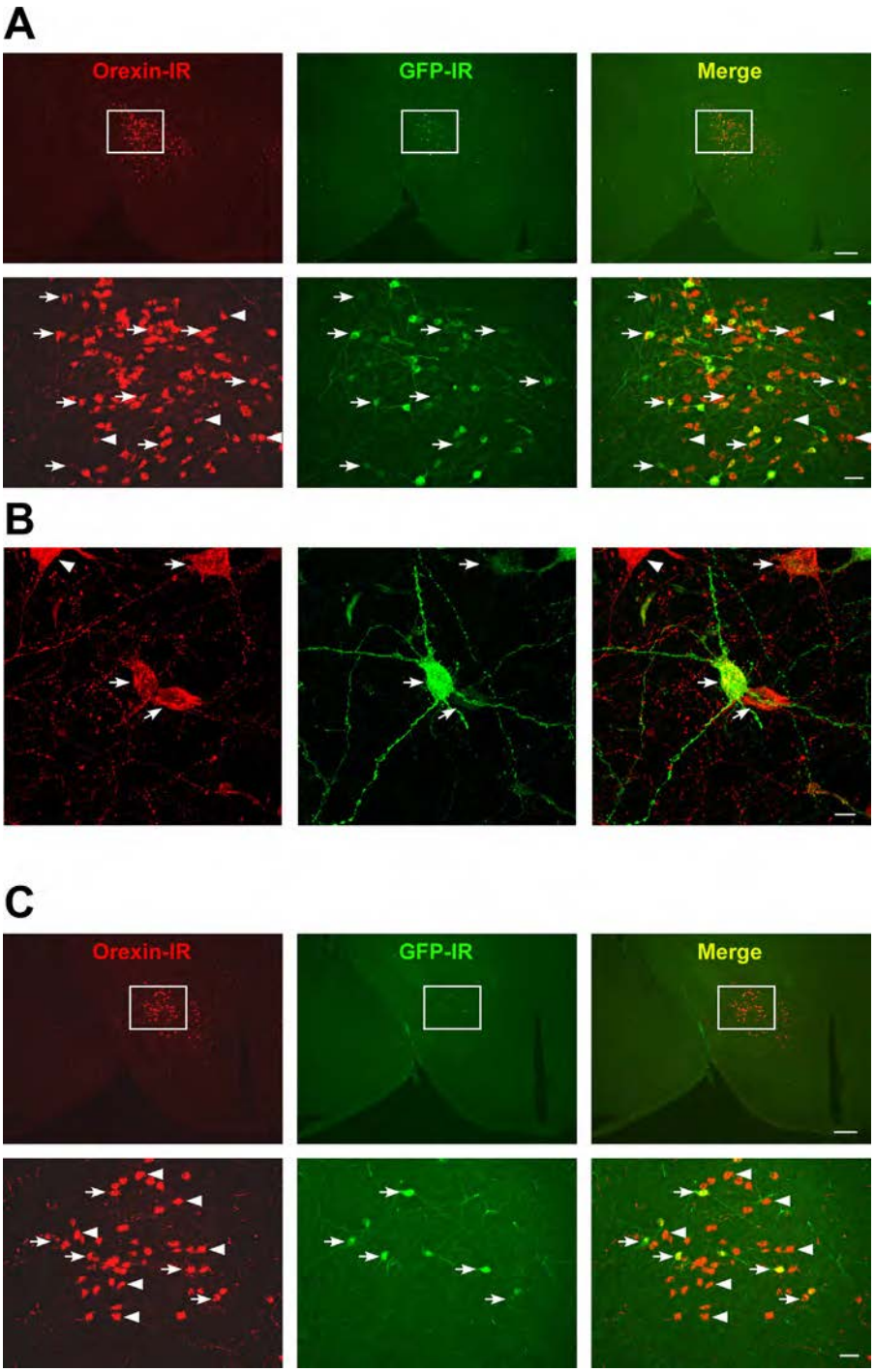

Fig. 2. ArchT is specifically expressed in orexin neurons in the *orexin-tTA; TetO ArchT* double-transgenic mouse brain. (A–C) Immunohistochemical analyses revealed the expression rate of two lines of *TetO ArchT* transgenic mice, line A (A) and line B (C). Orexin-IR neurons located in the LHA (Alexa594, red). GFP-IR neurons, indicating ArchT expression, are also observed in the LHA (Alexa488, green). The merged image shows specific expression of ArchT in orexin neurons in the LHA of *orexin-tTA; TetO ArchT* transgenic mice (upper panels, scale bar, 300 μm). In line A (A), 72.4 ± 12.2% ($n = 4$) of orexin neurons express ArchT. In line B (C) 23.9 ± 2.2% ($n = 3$) of orexin neurons express ArchT. No expression of ArchT outside of orexin neurons was observed throughout the brain in either transgenic mouse line. The lower panels are higher magnifications of the squared region in the upper panels (scale bar, 50 μm). (B) Confocal microscopic image of *orexin-tTA; TetO ArchT* (line A) mouse showing that ArchT expression is observed in the soma and dendrites of orexin neurons. Arrows indicate an example of GFP-expressing orexin neurons. Arrowheads indicate an example of GFP-non-expressing orexin neurons. Scale bar, 10 μm. (For interpretation of the references to color in this figure legend, the reader is referred to the web version of the article.)

meter (VEGA, Ophir Optronics Ltd., Wilmington, MA). Each animal's behavior was monitored through a CCD video camera and recorded on a computer synchronized with EEG and EMG recordings using the SleepSign video option system (Kissei Comtec). The infrared activity monitor was a sensor mounted on top of the cage to measure locomotor activity. The sensor's output signals representing the magnitude of each animal's movement were digitally converted and transferred to a computer.

Polysomnographic recordings were automatically scored offline, with each epoch scored as wakefulness, SWS, or REM sleep by SleepSign according to standard criteria [24,39]. All vigilance state classifications assigned by SleepSign were examined visually and corrected if necessary. To score sleep/wakefulness fragmentation during light illumination, the number of changes in sleep/wakefulness state, such as the transition from wakefulness to SWS, from SWS to REM sleep, from SWS to wakefulness, and from REM sleep to wakefulness, were counted as state transitions.

2.8. Statistical analysis

Data were analyzed by paired *t*-test, un-paired *t*-test, one-way ANOVA, or two-way ANOVA as appropriate for the parameters examined using KaleidaGraph 4.0 software (Hulinks, Tokyo, Japan). When appropriate, ANOVA tests were followed by *post hoc* analysis of significance using Fisher's Protected Least Significant Difference test. Probability (p)-values less than 0.05 were considered statistically significant.

3. Results

3.1. Specific expression of ArchT in orexin neurons

TetO ArchT BAC transgenic mice were generated in which ArchT-EGFP fusion protein was induced by using the tetracycline-controlled gene induction system. To achieve sufficient ArchT expression to make targeted cells hyperpolarize, we took advantage of the enhancing gene expression module; the *TetO* cassette was inserted downstream of β-actin gene allele, a housekeeping gene, in the BAC (Fig. 1A) [37]. A total of three *TetO ArchT* BAC transgene-positive founders were obtained (lines A–C). The transgene was transferred to the N1 generation of lines A and B, but not line C. tTA expression is driven by a specific promoter, in this case the human prepro-orexin promoter, resulting tTA expression in orexin neurons. Subsequently, tTA transactivates *ArchT-EGFP* induction by binding TetO sequences in orexin neurons (Fig. 1B). *TetO ArchT* mice (line A or B) were bred with *orexin-tTA* mice and *orexin-tTA; TetO ArchT* double-transgenic mice were used in this study (Fig. 1C).

The specific expression of ArchT (lines A and B) in orexin neurons was confirmed by double-labeled immunohistochemistry. An anti-GFP antibody was used to detect ArchT-EGFP fusion proteins in double-transgenic mice. Merged pictures (GFP-IR and orexin-IR) revealed that ArchT-EGFP was exclusively observed in orexin neurons of *orexin-tTA; TetO ArchT* (line A) (Fig. 2A and B) and *orexin-tTA; TetO ArchT* (line B) (Fig. 2C) mice. In both double-transgenic lines, we did not observe ArchT-EGFP expressing cells other than orexin neurons. Confocal microscopic observation revealed that ArchT was detected in the soma and dendrites of orexin neurons. Orexin neurons expressing ArchT did not show blebbing or other features indicative of inappropriate trafficking (Fig. 2B). The number and morphology of orexin-IR neurons in *orexin-tTA; TetO ArchT* (line A) transgenic mice were indistinguishable from those wild-type mice or monogenic littermate mice (*orexin-tTA* or *TetO ArchT* mice, data not shown), suggesting that ArchT expression is not toxic to orexin neurons. ArchT expression rates (GFP-IR/orexin-IR × 100%) in *orexin-tTA; TetO ArchT* (line A) and *orexin-tTA; TetO ArchT* (line B) mice was 72.4 ± 12.2% (n = 4) and 23.9 ± 2.2% (n = 3), respectively. *TetO ArchT* (line A) mice were used for the following *in vitro* and *in vivo* experiments since line A showed a significantly higher gene expression rate.

3.2. Green light illumination inhibits the activity of ArchT-expressing orexin neurons

To confirm the function of ArchT expressed in the transgenic mouse brain, slice patch clamp analyses were performed. Orexin neurons were whole cell current-clamped and green light (549 ± 7.5 nm) was illuminated, since previous reports revealed that ArchT exhibited the most potent sensitivity for yellow-green light illumination (around 570 nm) [36]. Green light was illuminated through an objective lens. Green light illumination (10% light intensity; 2.5 mW) instantaneously hyperpolarized the membrane potential and completely inhibited the generation of action potentials in orexin neurons for 30 s (Fig. 3A). After light cessation, the activity in silenced orexin neurons recovered ultimately to baseline firing rates without showing a rapid rebound activity. The magnitude of ArchT-mediated hyperpolarization depended on the light intensity in the presence of TTX (Fig. 3B). Green light illumination induced transient currents and sustained currents and these two were separately analyzed. Green light-induced hyperpolarizations immediately after light activation of orexin neurons (transient potential) were 4.1 ± 1.6 mV (n = 8, p = 0.77, not significantly different (NS), ANOVA), 20.7 ± 4.1 mV (n = 8, p = 0.08, NS, ANOVA), 35.1 ± 6.3 mV (n = 8, p = 0.002, ANOVA), 38.1 ± 6.7 mV (n = 8, p = 0.001, ANOVA), 43.4 ± 7.9 mV (n = 8, p < 0.001, ANOVA), 60.7 ± 9.8 mV (n = 10, p < 0.001, ANOVA), 72.2 ± 11.8 mV (n = 10, p < 0.001, ANOVA), 70.4 ± 11.8 mV (n = 10, p < 0.001, ANOVA) and 69.6 ± 11.7 mV (n = 10, p < 0.001, ANOVA) under light intensities of 1, 2, 3, 4, 5, 10, 25, 50 and 100% (25 mW), respectively (Fig. 3C). The magnitude of light-induced hyperpolarization showed a gradual decrease during light illumination. The hyperpolarizations just before light cessation (sustained) were 2.9 ± 1.1 mV (n = 8, p = 0.85, NS, ANOVA), 17.3 ± 4.0 mV (n = 8, p = 0.14, NS, ANOVA), 24.8 ± 4.4 mV (n = 8, p = 0.03, ANOVA), 26.1 ± 4.0 mV (n = 8, p = 0.02, ANOVA), 29.5 ± 4.7 mV (n = 8, p = 0.01, ANOVA), 42.8 ± 7.3 mV (n = 10, p < 0.001, ANOVA), 49.1 ± 8.0 mV (n = 10, p < 0.001, ANOVA), 49.1 ± 9.4 mV (n = 10, p < 0.001, ANOVA) and 48.7 ± 10.1 mV (n = 10, p < 0.001, ANOVA) under light intensities of 1, 2, 3, 4, 5, 10, 25, 50 and 100% (25 mW), respectively (Fig. 3C). In contrast, green light (100% intensity) had little effect on the membrane potential of EGFP-negative neurons in *orexin-tTA; TetO ArchT* mice (0.8 ± 0.9 mV, n = 9).

Under voltage clamp mode, green light was illuminated onto ArchT-expressing orexin neurons in the presence of TTX. At the holding membrane potential of −60 mV, green light illumination induced outward currents in a light intensity-dependent manner (Fig. 3D). Green light-induced transient outward currents were 5.0 ± 0.8 pA (n = 11, p = 0.90, NS, ANOVA), 23.7 ± 5.5 pA (n = 11, p = 0.51, NS, ANOVA), 51.7 ± 11.8 pA (n = 11, p = 0.15, NS, ANOVA), 67.7 ± 15.6 pA (n = 11, p = 0.06, NS, ANOVA), 80.6 ± 19.0 pA (n = 11, p = 0.02, ANOVA), 117.0 ± 28.9 pA (n = 12, p < 0.001, ANOVA), 165.7 ± 40.3 pA (n = 12, p < 0.001, ANOVA), 185.6 ± 45.6 pA (n = 12, p < 0.001, ANOVA), and 201.1 ± 49.7 pA (n = 12, p < 0.001, ANOVA) under light intensities of 1, 2, 3, 4, 5, 10, 25, 50 and 100% (25 mW), respectively (Fig. 3E). Sustained outward currents were 4.7 ± 0.8 pA (n = 11, p = 0.91, NS, ANOVA), 19.2 ± 3.8 pA (n = 11, p = 0.60, NS, ANOVA), 39.0 ± 8.3 pA (n = 11, p = 0.27, NS, ANOVA), 47.8 ± 9.5 pA (n = 11, p = 0.18, NS, ANOVA), 55.8 ± 10.9 pA (n = 11, p = 0.12, NS, ANOVA), 78.0 ± 15.5 pA (n = 12, p = 0.03, ANOVA), 96.5 ± 17.8 pA (n = 12, p = 0.006, ANOVA), 101.2 ± 17.8 pA (n = 12, p = 0.004, ANOVA) and 103.2 ± 16.9 pA (n = 12, p = 0.003, ANOVA) under light intensities of 1, 2, 3, 4, 5, 10, 25, 50 and 100% (25 mW), respectively (Fig. 3E).

Next, green light-induced inhibition of orexin neurons was confirmed using a loose cell-attached recording, which monitors firing frequency without affecting the intracellular conditions of the neuron being recorded. Before light illumination, orexin neurons exhibited spontaneous firing at a rate of 6.5 Hz. Long-lasting green light illumination (10%, 2.5 mW) for 10 min completely inhibited spontaneous firing in ArchT-expressing orexin neurons (Fig. 3F). Approximately 7 min after light termination, firing had recovered to basal levels although the neuronal activity remained attenuated for a few minutes, which was in agreement with the current clamp results. These results strongly suggest that light illumination of the hypothalamus would inhibit the activity of orexin neurons *in vivo*.

3.3. Inhibition of orexin neuronal activity by green light illumination in vivo

To confirm whether acute (1 min) silencing of orexin neuronal activity induces a transition from wakefulness to SWS in *orexin-tTA; TetO ArchT* mice, which have previously been described by our group using *orexin/Halo* mice [35], we performed *in vivo* 1-min

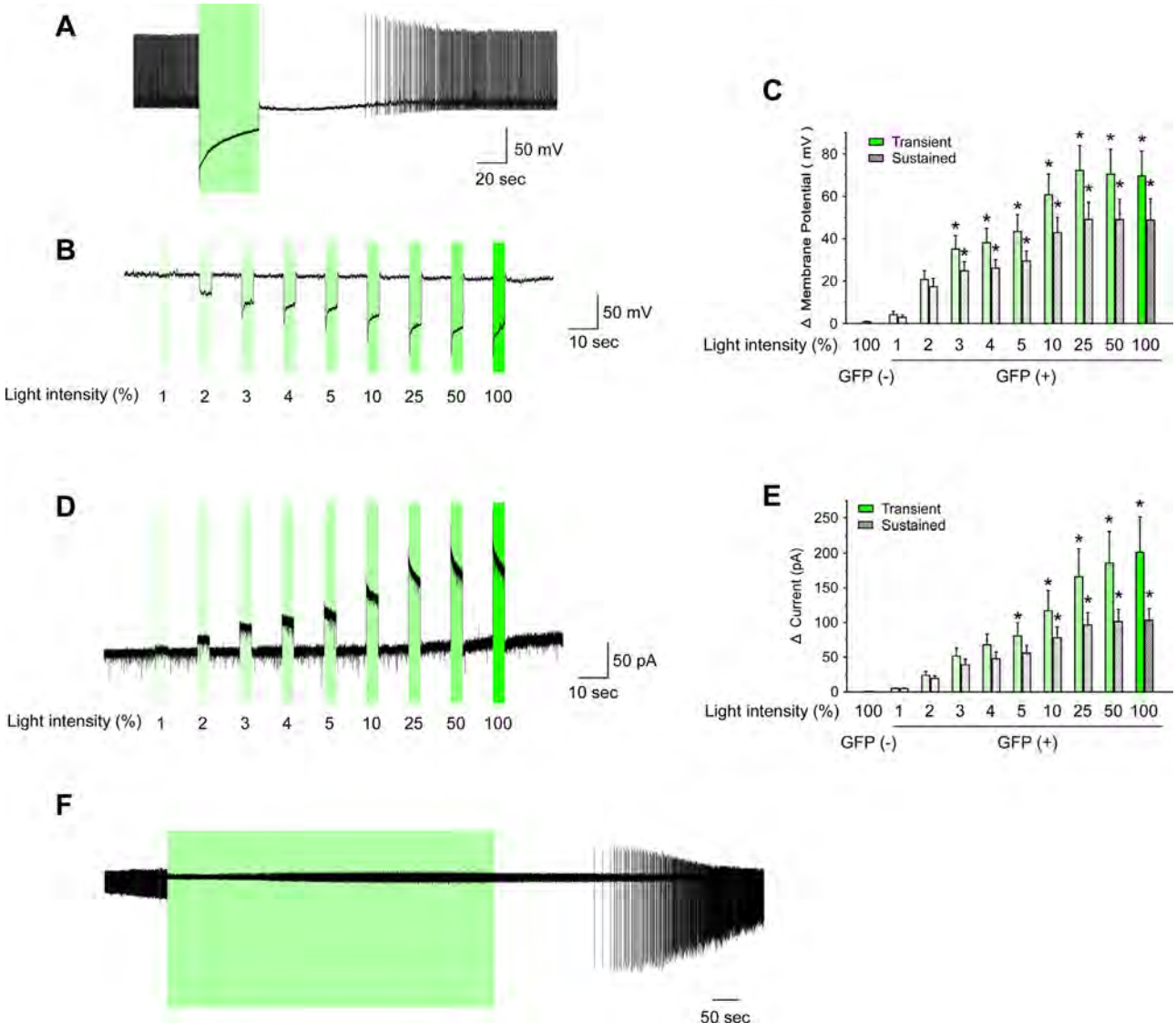

Fig. 3. Green light inhibits the activity of ArchT-expressing orexin neurons *in vitro*. (A) Under current-clamp mode, continuous green light (549 ± 7.5 nm) illumination for 30 s induced hyperpolarization and completely inhibited spontaneous action potentials in ArchT-expressing orexin neurons. (B) In the presence of TTX, green light produced hyperpolarizations in a light intensity-dependent manner. Light intensities were 1, 2, 3, 4, 5, 10, 25, 50 and 100% (23 mW), from left to right. (C) Bar graph summarizing the data in B. (D) Under whole-cell voltage-clamp mode, with membrane potential holding at −60 mV, green light induced outward currents in a light intensity-dependent manner in the presence of TTX. (E) Bar graph summarizing the data in D. (F) In a loose cell-attached recording from ArchT-expressing orexin neurons, continuous green light illumination for 10 min also completely inhibited spontaneous firing. Green light was applied through an objective lens for a duration indicated by the green bars. Values represent means ± S.E.M. $^*p < 0.05$ *vs.* 100% green light illumination of EGFP (−) neurons. Transient, transient potential or current was observed immediately after light onset. Sustained, sustained potential or current was observed just before light cessation. (For interpretation of the references to color in this figure legend, the reader is referred to the web version of the article.)

photic illumination within the hypothalamus using freely moving mice. To determine sleep/wakefulness states during recording, mice were chronically implanted with EEG and EMG electrodes. To deliver green light to the hypothalamus, plastic fiber optics were bilaterally implanted into the brain. During the time when mice displayed spontaneous wakefulness in the late light period (13:00–19:00), green light was illuminated at random for 1 min through the fiber optics from a light source (542 ± 13.5 nm). During green light illumination into the hypothalamus, EEG power gradually increased and EMG power gradually decreased, suggesting an induction of SWS (Fig. 4A). After about 40 s from light on, all *orexin-tTA; TetO ArchT* transgenic mice exhibited SWS but not REM sleep ($n = 12$, Fig. 4B–D). In contrast, in the dark period (21:00–0:00), during which nocturnal mice have the greatest spontaneous activity and arousal levels, green light illumination into the hypothalamus had no effect on sleep/wakefulness patterns in freely-moving *orexin-tTA; TetO ArchT* transgenic mice ($n = 11$, Fig. 4E–H). These results are in agreement with our previous results [35].

3.4. *In vivo green light illumination of the hypothalamus increases time spent in slow wave sleep during the dark period but not during the light period*

Next, to confirm whether green light illumination could inhibit the activity of orexin neurons *in vivo*, double immunohistochemical staining for c-Fos and orexin was performed. To deliver green light into the hypothalamus, plastic fiber optics were bilaterally implanted into the brain of *orexin-tTA; TetO ArchT* mice. Green light was illuminated for 1 h during the dark period (20:00–21:00), at the time of day when orexin neuronal activity is maximal. Subsequently, the animals were sacrificed and the brains were fixed at

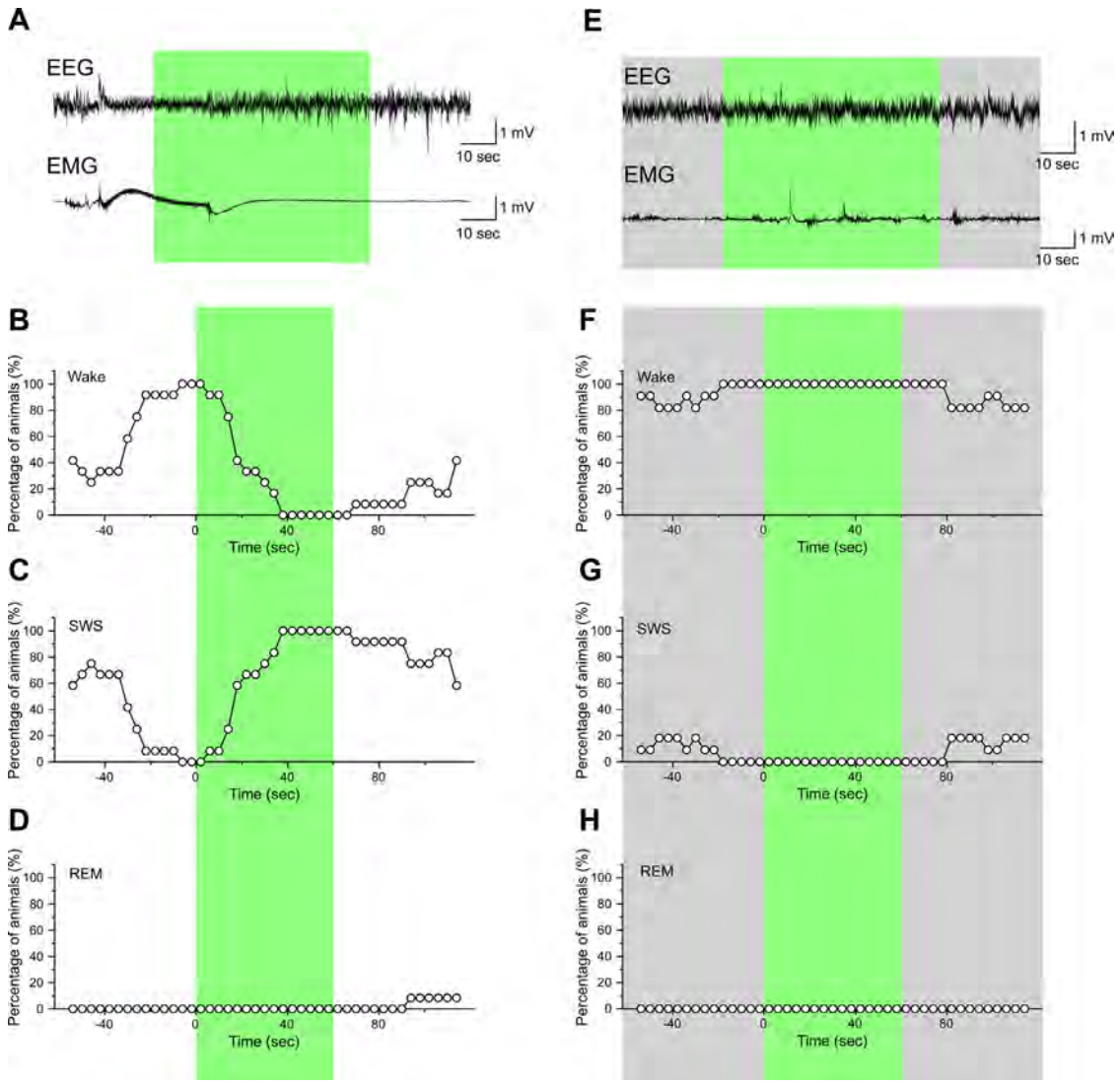

Fig. 4. Acute optogenetic inhibition of orexin neurons *in vivo* induces SWS in *orexin-tTA; TetO ArchT* mice. EEG and EMG electrodes were chronically implanted to determine sleep/wakefulness states. Plastic fiber optics (0.5 mm diameter) were bilaterally inserted above the hypothalamus. Green light from a Lumencor (542 ± 13.5 nm) was applied through the fiber optics for 60 s. (A and E) Representative traces show EEG (upper trace) and EMG (lower trace) during green light illumination during the second half of the light period (13:00–19:00) (A) and during the dark period (20:00–0:00) (E). Green light illumination was initiated at random when *orexin-tTA; TetO ArchT* mice had been awake for at least 8 s (2 epochs) during either the light or dark period. Line graphs summarize the percentage of animals exhibiting wakefulness (B and F), SWS (C and G), and REM sleep (D and H) during green light illumination. Wake; wakefulness. (For interpretation of the references to color in this figure legend, the reader is referred to the web version of the article.)

21:00. *Orexin-tTA; TetO ArchT* mice without green light illumination were used as controls.

In the control group (without light illumination), several double-labeled neurons (orexin-positive neurons with c-Fos-positive nuclei) are observed (Fig. 5A, arrowheads). The c-Fos expression rate (orexin-IR with c-Fos-IR/orexin-IR × 100%) in control mice was 30.5 ± 1.9% (n = 11) (Fig. 5B). Comparatively, the c-Fos expression rate in the 1 h green light illumination group was significantly decreased to 13.2 ± 1.9% (Fig. 5A and B, n = 10, $p < 0.001$, un-paired t-test). These observations demonstrated that continuous green light illumination for 1 h appropriately inhibited the activity of orexin neurons of *orexin-tTA; TetO ArchT* mice.

To study the physiological significance of orexin neuronal activity in the regulation of sleep/wakefulness, we performed *in vivo* long-lasting green light illumination using freely moving *orexin-tTA; TetO ArchT* mice. Based on the results of c-Fos immunostaining, continuous 1 h green light illumination was applied (Fig. 6A). First, we examined the effect of green light illumination during the dark period when nocturnal mice have the greatest spontaneous activity and arousal levels (20:00–21:00) (Fig. 6B). *Orexin-tTA; TetO ArchT* mice without light illumination were used as controls. A typical hypnogram of a control mouse shows that the mouse spent most of the time awake at the beginning of the dark period (Fig. 6Ba). In contrast, a mouse receiving green light illumination frequently transitioned to SWS (Fig. 6Bb). The total time spent in SWS during green light illumination was significantly increased compared with that of control mice (Fig. 6Bc). In the control mice, the total time in wakefulness, SWS and REM sleep over 1 h was 50.7 ± 3.0 min (wakefulness, n = 7), 9.1 ± 3.0 min (SWS, n = 7) and 0.2 ± 0.1 min (REM, n = 7), respectively. In the green light-illuminated group, the total time in wakefulness, SWS and REM sleep over 1 h was 40.7 ± 4.1 min (wakefulness, n = 7, p = 0.049, paired t-test), 9.1 ± 3.0 min (SWS, n = 7, p = 0.048, paired t-test) and 0.3 ± 0.2 min (REM, n = 7, p = 0.94, NS, paired t-test), respectively. These results suggested that inhibition of orexin neuronal activity resulted in an increased time spent

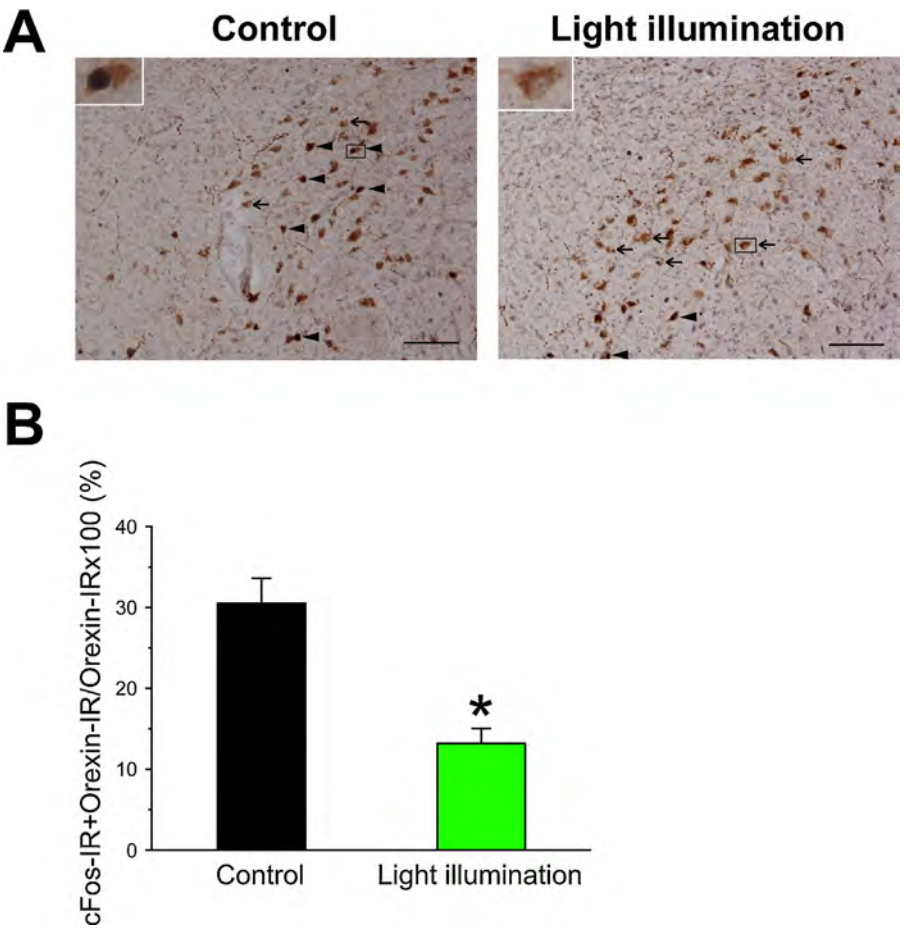

Fig. 5. Inhibition of orexin neurons by green light illumination *in vivo*. *Orexin-tTA; TetO ArchT* transgenic mice were decapitated during the dark period, at 21:00. The light illumination group received green light into the hypothalamus for 1 h (from 20:00 to 21:00) before decapitation. Green light was applied through plastic fiber optics (diameter of 0.5 mm) that were bilaterally inserted into the hypothalamus. Coronal sections through the hypothalamus containing orexin neurons were studied using double immunostaining. (A) Immunoreactivity for orexin (brown) located in the LHA. Immunoreactivity for c-Fos (black) was observed throughout the brain. Arrowheads indicate c-Fos- and orexin-double positive neurons (arrowheads). Arrows indicate c-Fos-negative and orexin-positive neurons. Insets are higher magnifications of the squared region. Scale bars 100 μm. (B) Bar graph summarizing the data in (A) shows the expression rate of c-Fos in orexin neurons. The black bar indicates the condition without light illumination and the green bar indicates the condition with 1 h light illumination before decapitation. Values are represented as means ± S.E.M. *, $p < 0.05$ *vs.* control in *orexin-tTA; TetO ArchT* transgenic mice. (For interpretation of the references to color in this figure legend, the reader is referred to the web version of the article.)

in SWS, accompanied by decreased time spent awake in the early dark period. Sleep/wakefulness state transition frequency in control mice was 6.9 ± 1.5 ($n = 7$), whereas the frequency in light-illuminated mice was 16.7 ± 3.3 ($n = 7$, $p = 0.019$, paired *t*-test) (Fig. 6Be). However, locomotor activity was not significantly altered: locomotor activity of control and light-illuminated groups was 1455.3 ± 210.8 counts ($n = 7$) and 1087.7 ± 185.4 counts ($n = 7$, $p = 0.12$, NS, paired *t*-test), respectively (Fig. 6Bd). These results suggest that the increase in the fragmentation of sleep/wakefulness cycles, which represents the dominant clinical manifestation of narcolepsy, is modeled by the inability to maintain consolidated wakefulness during light illumination in *orexin-tTA; TetO ArchT* mice.

Next, we examined the effect of a 1 h light illumination during the light period (12:00–13:00) (Fig. 6C). Mice are nocturnal animals, and are largely inactive in the light period. They spend most of their time sleeping during the light period (Fig. 6Ca). Green light illumination during the light period did not affect sleep/wakefulness patterns. They showed almost the same sleep/wakefulness patterns as control mice (Fig. 6Ca and Cb). There were no significant differences in total times of sleep/wakefulness states between light-illumination and no-illumination control groups (Fig. 6Cc). Without photic illumination, the total time in wakefulness, SWS and REM sleep was 12.2 ± 4.3 min ($n = 5$), 44.5 ± 4.3 min ($n = 5$) and 3.4 ± 0.5 min ($n = 5$), respectively. Following green light illumination for 1 h, the total time in wakefulness, SWS and REM sleep was 14.8 ± 6.5 min ($n = 5$, $p = 0.64$, NS, paired *t*-test), 43.2 ± 5.7 min ($n = 5$, $p = 0.80$, NS, paired *t*-test) and 2.1 ± 1.3 min ($n = 5$, $p = 0.37$, NS, paired *t*-test), respectively. In accordance with these results, locomotor activity and behavioral state transition frequency was not significantly different between groups ($n = 5$, Fig. 6Cd and Ce). These results suggest that inhibition of orexin neuron activity induced fragmentation of sleep/wakefulness in the dark period, but not in the light period.

4. Discussion

4.1. TetO ArchT mice are useful for sustained inhibition in vivo

Optogenetics is a powerful tool to study the regulatory mechanisms of behavior. Although activation of neurons using ChR2 often succeeded in controlling an animal's behavior, few studies have succeed in modifying behavior by silencing neurons. Previously, we used halorhodopsin (HaloR) to inhibit the activity of orexin neurons and found that inhibition of orexin neurons induced SWS when the mice were awake [35]. However, silencing through HaloR was insufficient to completely inhibit the activity of neurons and it was difficult to inhibit activity for more than 1 min, likely due to

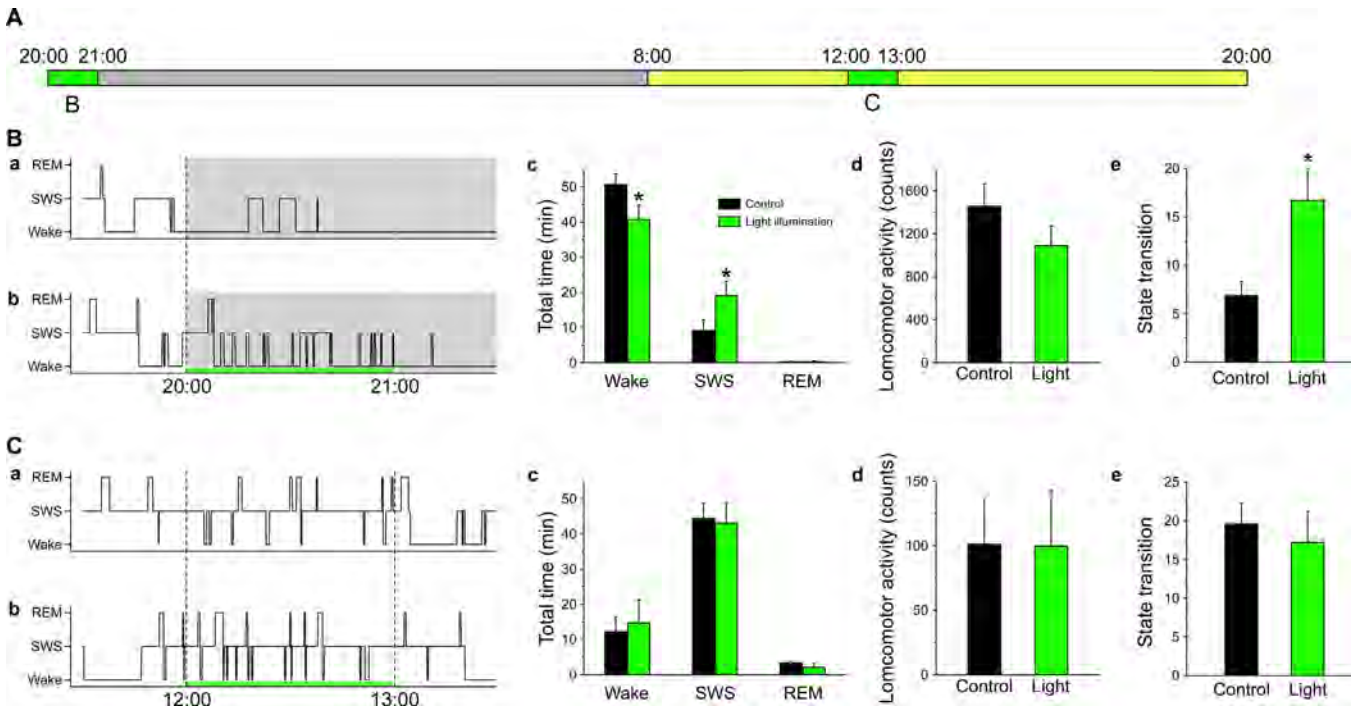

Fig. 6. Green light illumination increases time spent in SWS during the dark period. (A) Illustration showing the timing of the 1 h continuous illumination *in vivo*. *Orexin-tTA; TetO ArchT* mice were housed under controlled lighting conditions (12 h light/dark cycle; light on 8:00–20:00). These mice were illuminated during 20:00–21:00 (dark period) or during 12:00–13:00 (light period). Each mouse received photic illumination with an interval of at least 2 days between each illumination. (B) The results of 1 h green light illumination from 20:00 to 21:00. Shown are representative 2 h (19:30–21:30) hypnograms for the basal condition (Ba) and after a 1 h light illumination (Bb) of an *orexin-tTA; TetO ArchT* transgenic mouse during the dark period. Hypnograms were obtained by simultaneous EEG/EMG recording. Green light was applied through plastic fiber optics (diameter of 0.5 mm) that were bilaterally inserted into the hypothalamus. The green bar indicates the duration of light illumination. (Bc, Bd and Be) Bar graphs summarizing the data in (Ba) and (Bb): (Bc) total time spent in each vigilance state; (Bd) locomotor activity; (Be) the number of state transitions. (C) The results of a 1 h green light illumination from 12:00 to 13:00. Representative 2 h (11:30–13:30) hypnograms for the basal condition (Ca) and after 1 h light illumination (Cb) of an *orexin-tTA; TetO ArchT* transgenic mouse during the light period. (Cc, Cd and Ce) Bar graphs summarizing the data in (Ca) and (Cb): (Cc) total time spent in each vigilance state; (Cd) locomotor activity; (Ce) number of state transitions. Wake; wakefulness. Light; Light illumination. Values are represented as means ± S.E.M. *, $p < 0.05$ *vs.* control in *orexin-tTA; TetO ArchT* transgenic mice. (For interpretation of the references to color in this figure legend, the reader is referred to the web version of the article.)

desensitization mechanisms, at least in orexin neurons. To control instinctive behavior, such as sleep/wakefulness state in mice, it is essential to manipulate the activity of neurons for longer periods. ArchT, a green light-driven proton pump, produced strong and long lasting inhibition compared with HaloR. Prolonged manipulation of orexin neuronal activity seems vital to understand the neuronal circuitry underlying the maintenance of sleep/wakefulness in addition to the initiation of sleep/wakefulness.

In the present study, we generated a new line of transgenic mice, *TetO ArchT* BAC transgenic mice, which enable expression of ArchT in a specific cell type following breeding with *tTA* mice, in which a specific promoter drives tTA expression. We used the Tet system based on our previous report that this system can amplify the expression levels of transgene compared to direct expression using cell-type specific promoters [37]. High expression levels of light-activated proteins are important to achieve a significant manipulation of membrane potential, particularly in silencing neurons. The utility of using the Tet transgenic system for optogenetic manipulation was exemplified by the KENGE-tet system, employing *TetO ChR2 (C128S)* mice. The specific expression of ChR2 (C128S) was observed in Ca^{2+}-calmodulin-dependent protein kinase II (αCaMKII)-expressing neurons, 5-hydroxytryptamine receptor 5B (Htr5B)-expressing neurons, GABAergic neurons, astrocytes, oligodendrocytes and microglia when crossing with *αCaMKII-tTA* mice, *Htr5B-tTA* mice, *GAD67-tTA* mice, *Mlc1-tTA* mice, *PLP-tTA* mice and *Iba1-tTA* mice, respectively [37]. The generation of *TetO ArchT* mice further expands the researchers toolbox to inhibit various types of cells. To demonstrate the usefulness of *TetO ArchT* BAC transgenic mice, these animals were bred with *orexin-tTA* mice. Immunohistochemical data revealed that ArchT was expressed in more than 70% of orexin neurons with no ectopic expression in non-orexin neurons in the *orexin-tTA; TetO ArchT* double-transgenic mouse brain.

In vitro slice patch clamp recordings demonstrated that green light illumination instantaneously induced hyperpolarization or outward current in ArchT-expressing orexin neurons repetitively and in a light intensity-dependent manner. Silencing of orexin neurons was further confirmed by using a loose cell-attached recording, which records firing frequency without affecting intracellular conditions of the recorded neuron. In this recording condition, green light illumination for 10 min enabled a complete silencing of ArchT-expressing orexin neurons, suggesting a probability of inhibiting activity of orexin neurons *in vivo*. This implication was strongly supported by our immunohistochemical data for c-Fos, a marker of neuronal activity. Continuous 1 h green light illumination from the start of the dark period significantly decreased the number of orexin neurons expressing c-Fos, suggesting that orexin neuronal activity was inhibited *in vivo*. These results indicate that ArchT is a more potent silencer for long-lasting manipulation compared with HaloR, at least in orexin neurons.

4.2. Inhibition of orexin neuronal activity increases time spent in SWS only during the dark period

In this study, we demonstrated that acute (1 min) optogenetic inhibition of orexin neurons through ArchT increased transit probability from wakefulness to SWS in the light period, but failed in the dark period, in good agreement with our previous report using HaloR [35]. In contrast, the present study showed that 1 h optogenetic inhibition of orexin neurons through ArchT increased time spent in SWS and decreased time spent in wakefulness in

the dark period, but showed little effect on sleep/wakefulness in the light period. Why does this differential result arise? One possibility is that HaloR-induced inhibition was too weak to completely block the activity of orexin neurons during the dark period. Currents induced by ArchT (sustained current) are 20 times greater than those mediated by HaloR in orexin neurons. ArchT might completely inhibit the activity of orexin neurons even in the early dark period when orexin neurons are supposed to receive many excitatory inputs and to be highly active. The other possible factor is length of inhibition time. Likely due to desensitization mechanisms, HaloR could only produce inhibition for 1 min. Inhibition for such a limited period might be insufficient to induce sleep in the active period since a 1 min inhibition of orexin neurons during the dark period also had little effect on sleep/wakefulness patterns in *orexin/Archaerhodopsin-3(Arch)* transgenic mice. *Orexin/Arch* mice directly drive Arch expression in orexin neurons using a prepro-orexin promoter and inhibit orexin neurons with strength comparable to HaloR (unpublished data). Previous studies reported that CSF orexin levels in rats display a high peak during the dark period and lowest levels during the light period [40]. Therefore, 1 min silencing might not affect sleep/wakefulness patterns since orexin peptide concentrations are high in the CSF in the dark period. Comparatively, 1 h silencing of orexin neurons during the light period had little effect. This result is in agreement with previous reports demonstrating that orexin neuronal activity is necessary for the maintenance of wakefulness states rather than generating a waking state since orexin neuron-ablated mice and human narcolepsy patients have impairments in maintaining wakefulness but they can awaken. Mice are nocturnal animals that spend most of their time sleeping during the light period, but also frequently show brief waking episodes similar to a fragmentation of sleep/wakefulness. Thus, silencing for 1 h might not have induced further fragmentation within the light period.

The present study revealed that 1 h continuous optogenetic illumination in the dark period induced a fragmentation of the sleep/wakefulness cycle similar to mice lacking the orexin gene, the OX2R gene, orexin neurons and dogs with null mutations in orexin signaling [3–6]. However, inhibition of orexin neurons through ArchT did not induce a cataplexy-like behavioral arrest and direct transition from wakefulness to REM sleep. These behaviors are observed in prepro-orexin knockout mice and orexin neuron-ablated mice. These differences in phenotype might be related to the percentage of ArchT-expressing orexin neurons in our study. Immunohistochemical data revealed that ArchT was expressed in 72% of orexin neurons. In accordance with this result, 13% of orexin neurons still expressed c-Fos in the dark period even when orexin neurons were inhibited by green light illumination in *orexin-tTA; TetO ArchT* mice. These results indicate that activation of a small number of orexin neurons might be sufficient to protect a direct transition from wakefulness to REM sleep and cataplexy-like behavior. Another possibility is that reconstruction of neuronal networks after the loss of orexin neurons or loss of orexin signal might be necessary to trigger these symptoms. Similar results are observed in rats, dogs and humans that are orally administered the dual orexin receptor (OX1R and OX2R) antagonist, almorexant [41]. Pharmacological blockage of orexin receptors during the active period increased SWS and REM sleep and decreased wakefulness without evidence of cataplectic symptoms or direct transition from wakefulness to REM sleep.

5. Conclusions

In this study, we generated a novel line of *TetO ArchT* BAC transgenic mice. Data from *Orexin-tTA; TetO ArchT* double-transgenic mice confirmed that ArchT is correctly expressed and functions to inhibit the activity of tTA-expressing neurons. Long-lasting silencing of orexin neurons *in vivo* increased time spent in SWS and decreased time spent awake during the dark period but not during the light period, indicating the physiological importance of orexin neuronal activity in the maintenance of arousal during the active phase.

Acknowledgements

This study was supported by the JST PRESTO program, Grant-in-Aid for Scientific Research on Innovative Areas “Mesoscopic Neurocircuitry” (23115103), Grant-in-Aid for Scientific Research (B) (23300142) (A.Y.), a Japan Society for Promotion of Science postdoctoral fellowship (T.T.).We thank Dr. A. Inutsuka for confocal microscopic observation, C. Saito and K. Nishimura for technical assistance.

References

[1] Sakurai T, Amemiya A, Ishii M, Matsuzaki I, Chemelli RM, Tanaka H, et al. Orexins and orexin receptors: a family of hypothalamic neuropeptides and G protein-coupled receptors that regulate feeding behavior. Cell 1998;92:573–85.
[2] de Lecea L, Kilduff TS, Peyron C, Gao X, Foye PE, Danielson PE, et al. The hypocretins: hypothalamus-specific peptides with neuroexcitatory activity. Proceedings of the National Academy of Sciences of the United States of America 1998;95:322–7.
[3] Hara J, Beuckmann CT, Nambu T, Willie JT, Chemelli RM, Sinton CM, et al. Genetic ablation of orexin neurons in mice results in narcolepsy, hypophagia, and obesity. Neuron 2001;30:345–54.
[4] Chemelli RM, Willie JT, Sinton CM, Elmquist JK, Scammell T, Lee C, et al. Narcolepsy in orexin knockout mice: molecular genetics of sleep regulation. Cell 1999;98:437–51.
[5] Lin L, Faraco J, Li R, Kadotani H, Rogers W, Lin X, et al. The sleep disorder canine narcolepsy is caused by a mutation in the hypocretin (orexin) receptor 2 gene. Cell 1999;98:365–76.
[6] Willie JT, Chemelli RM, Sinton CM, Tokita S, Williams SC, Kisanuki YY, et al. Distinct narcolepsy syndromes in Orexin receptor-2 and Orexin null mice: molecular genetic dissection of Non-REM and REM sleep regulatory processes. Neuron 2003;38:715–30.
[7] Nishino S, Ripley B, Overeem S, Lammers GJ, Mignot E. Hypocretin (orexin) deficiency in human narcolepsy. Lancet 2000;355:39–40.
[8] Peyron C, Faraco J, Rogers W, Ripley B, Overeem S, Charnay Y, et al. A mutation in a case of early onset narcolepsy and a generalized absence of hypocretin peptides in human narcoleptic brains. Nature Medicine 2000;6:991–7.
[9] Thannickal TC, Moore RY, Nienhuis R, Ramanathan L, Gulyani S, Aldrich M, et al. Reduced number of hypocretin neurons in human narcolepsy. Neuron 2000;27:469–74.
[10] Hagan JJ, Leslie RA, Patel S, Evans ML, Wattam TA, Holmes S, et al. Orexin A activates locus coeruleus cell firing and increases arousal in the rat. Proceedings of the National Academy of Sciences of the United States of America 1999;96:10911–6.
[11] Piper DC, Upton N, Smith MI, Hunter AJ. The novel brain neuropeptide, orexin-A, modulates the sleep-wake cycle of rats. European Journal of Neuroscience 2000;12:726–30.
[12] Lee MG, Hassani OK, Jones BE. Discharge of identified orexin/hypocretin neurons across the sleep-waking cycle. Journal of Neuroscience 2005;25:6716–20.
[13] Mileykovskiy BY, Kiyashchenko LI, Siegel JM. Behavioral correlates of activity in identified hypocretin/orexin neurons. Neuron 2005;46:787–98.
[14] Takahashi K, Lin JS, Sakai K. Neuronal activity of orexin and non-orexin waking-active neurons during wake-sleep states in the mouse. Neuroscience 2008;153:860–70.
[15] Nambu T, Sakurai T, Mizukami K, Hosoya Y, Yanagisawa M, Goto K. Distribution of orexin neurons in the adult rat brain. Brain Research 1999;827:243–60.
[16] Peyron C, Tighe DK, van den Pol AN, de Lecea L, Heller HC, Sutcliffe JG, et al. Neurons containing hypocretin (orexin) project to multiple neuronal systems. Journal of Neuroscience 1998;18:9996–10015.
[17] McGinty DJ, Harper RM. Dorsal raphe neurons: depression of firing during sleep in cats. Brain Research 1976;101:569–75.
[18] Chu NS, Bloom FE. Activity patterns of catecholamine-containing pontine neurons in the dorso-lateral tegmentum of unrestrained cats. Journal of Neurobiology 1974;5:527–44.
[19] Hobson JA, McCarley RW, Wyzinski PW. Sleep cycle oscillation: reciprocal discharge by two brainstem neuronal groups. Science 1975;189:55–8.
[20] Takahashi K, Lin JS, Sakai K. Neuronal activity of histaminergic tuberomammillary neurons during wake-sleep states in the mouse. Journal of Neuroscience 2006;26:10292–8.

[21] Bayer L, Eggermann E, Serafin M, Saint-Mleux B, Machard D, Jones B, et al. Orexins (hypocretins) directly excite tuberomammillary neurons. European Journal of Neuroscience 2001;14:1571–5.
[22] Horvath TL, Peyron C, Diano S, Ivanov A, Aston-Jones G, Kilduff TS, et al. Hypocretin (orexin) activation and synaptic innervation of the locus coeruleus noradrenergic system. Journal of Comparative Neurology 1999;415:145–59.
[23] Sakurai T. The neural circuit of orexin (hypocretin): maintaining sleep and wakefulness. Nature Reviews Neuroscience 2007;8:171–81.
[24] Yamanaka A, Tsujino N, Funahashi H, Honda K, Guan JL, Wang QP, et al. Orexins activate histaminergic neurons via the orexin 2 receptor. Biochemical and Biophysical Research Communications 2002;290:1237–45.
[25] Chou TC, Bjorkum AA, Gaus SE, Lu J, Scammell TE, Saper CB. Afferents to the ventrolateral preoptic nucleus. Journal of Neuroscience 2002;22:977–90.
[26] Gallopin T, Fort P, Eggermann E, Cauli B, Luppi PH, Rossier J, et al. Identification of sleep-promoting neurons in vitro. Nature 2000;404:992–5.
[27] Morairty S, Rainnie D, McCarley R, Greene R. Disinhibition of ventrolateral preoptic area sleep-active neurons by adenosine: a new mechanism for sleep promotion. Neuroscience 2004;123:451–7.
[28] Sakurai T, Nagata R, Yamanaka A, Kawamura H, Tsujino N, Muraki Y, et al. Input of orexin/hypocretin neurons revealed by a genetically encoded tracer in mice. Neuron 2005;46:297–308.
[29] Yamanaka A, Beuckmann CT, Willie JT, Hara J, Tsujino N, Mieda M, et al. Hypothalamic orexin neurons regulate arousal according to energy balance in mice. Neuron 2003;38:701–13.
[30] Xie X, Crowder TL, Yamanaka A, Morairty SR, Lewinter RD, Sakurai T, et al. GABA(B) receptor-mediated modulation of hypocretin/orexin neurones in mouse hypothalamus. Journal of Physiology 2006;574:399–414.
[31] Lu J, Bjorkum AA, Xu M, Gaus SE, Shiromani PJ, Saper CB. Selective activation of the extended ventrolateral preoptic nucleus during rapid eye movement sleep. Journal of Neuroscience 2002;22:4568–76.
[32] Adamantidis AR, Zhang F, Aravanis AM, Deisseroth K, de Lecea L. Neural substrates of awakening probed with optogenetic control of hypocretin neurons. Nature 2007;450:420–4.
[33] Carter ME, Adamantidis A, Ohtsu H, Deisseroth K, de Lecea L. Sleep homeostasis modulates hypocretin-mediated sleep-to-wake transitions. Journal of Neuroscience 2009;29:10939–49.
[34] Tsunematsu T, Tanaka KF, Yamanaka A, Koizumi A. Ectopic expression of melanopsin in orexin/hypocretin neurons enables control of wakefulness of mice in vivo by blue light. Neuroscience Research 2012;75(1):23–8.
[35] Tsunematsu T, Kilduff TS, Boyden ES, Takahashi S, Tominaga M, Yamanaka A. Acute optogenetic silencing of orexin/hypocretin neurons induces slow-wave sleep in Mice. Journal of Neuroscience 2011;31:10529–39.
[36] Han X, Chow BY, Zhou H, Klapoetke NC, Chuong A, Rajimehr R, et al. A high-light sensitivity optical neural silencer: development and application to optogenetic control of non-human primate cortex. Frontiers in Systems Neuroscience 2011;5:18.
[37] Tanaka KF, Matsui K, Sasaki T, Sano H, Sugio S, Fan K, et al. Expanding the repertoire of optogenetically targeted cells with an enhanced gene expression system. Cell Reports 2012;2(2):397–406.
[38] Tabuchi S, Tsunematsu T, Kilduff TS, Sugio S, Tanaka KF, Takahashi S, et al. Influence of inhibitory serotonergic inputs to orexin/hypocretin neurons on the diurnal rhythm of sleep and wakefulness. Sleep, in press.
[39] Tobler I, Deboer T, Fischer M. Sleep and sleep regulation in normal and prion protein-deficient mice. Journal of Neuroscience 1997;17:1869–79.
[40] Yoshida Y, Fujiki N, Nakajima T, Ripley B, Matsumura H, Yoneda H, et al. Fluctuation of extracellular hypocretin-1 (orexin A) levels in the rat in relation to the light-dark cycle and sleep-wake activities. The European Journal of Neuroscience 2001;14:1075–81.
[41] Brisbare-Roch C, Dingemanse J, Koberstein R, Hoever P, Aissaoui H, Flores S, et al. Promotion of sleep by targeting the orexin system in rats, dogs and humans. Nature Medicine 2007;13:150–5.